Colloid and Polymer Science (2019) 297:821–830
https://doi.org/10.1007/s00396-019-04512-7

ORIGINAL CONTRIBUTION

Nanocomposite interpenetrating hydrogels with high toughness and good self-recovery

Huijuan Zhang[1] · Xue Wang[1] · Huanxuan Huang[1] · Biao Yang[1] · Chun Wang[1] · Hui Sun[1]

Received: 17 February 2019 / Revised: 3 April 2019 / Accepted: 5 April 2019 / Published online: 24 April 2019

Abstract

It is particularly desirable to fabricate highly tough hydrogels with excellent self-recoverable properties for applications where high stress is required. In this work, we prepared a tough, fast self-recoverable nanocomposite hydrogel by chemical cross-linking of acrylamide (AM) monomers with vinyl-modified silica nanoparticles (VSNPs), combined with physical cross-linking of polyvinyl alcohol (PVA). The uniaxial tensile test showed that the nanocomposite hydrogel has excellent mechanical properties. The maximum elongation at break was as high as 666%, and the tensile strength was as high as 1.68 MPa. Cyclic loading-unloading tests revealed the excellent self-healing properties of the nanocomposite hydrogel. It is worth noting that the nanocomposite hydrogel exhibited higher strength after two loading-unloading cycles, due to the orientation of the PVA when stretched. In addition, the effects of PVA, VSNPs, and AM concentrations, and the number of PVA freeze-thaw cycles and freezing duration on the mechanical properties of the hydrogels were investigated in detail.

Keywords PVA · Nanocomposite interpenetrating hydrogel · Toughness · Self-recovery · Draw-induced strengthening

Introduction

Polymeric hydrogels are three-dimensional networks, which are attractive in diverse fields, i.e., drug delivery [1, 2], tissue engineering [3], and actuators [4], owing to their promising biocompatibility and stimuli-responsiveness endowed by the network components. In many cases, however, the scope of applications is largely constrained due to the unsatisfactory mechanical strength. To address the shortcomings, representative methods including double network gels [5–9], topological gels [10], nanocomposite gels [11–14], and hybrid gels [15, 16] have been developed either by optimizing the network structures or by introducing a multifunctional cross-linker. These hydrogels exhibited excellent mechanical properties, such as high toughness and high deformability, when compared with traditional hydrogels [17–22].

In nanocomposite gels, for example, the gels are formed by initiating polymerization from the clay surface, and the flexible polymer chains on the surface were not restricted and thus exhibited superior elongation and good recovery. In addition to the laminated nanomaterials, i.e., clay [23–25], montmorillonite [26], graphene oxide [27–29], nanoparticles [30] were also employed as reinforcement. In this regard, Xie group developed a method to prepare tough nanocomposite hydrogels, by initiating polymerization of acrylamide (AM) monomers on the surface of vinyl hybrid silica nanoparticles (VSNP) [31]. The intermolecular hydrogen bonding in polyacrylamide (PAM) chains and the VSNP transfer center collaboratively contributed to the good mechanical performance of the VSNP hydrogel. The tensile strength was 73–313 kPa with elongation at break of 1210–3420%. Further investigation to include ferric ion-mediated ionic interactions between poly(acrylic) acid (PAA) polymer chains in PAA/VSNP hydrogel can reach tensile strength of 860 kPa [32]. Nevertheless, the strength is still unsatisfactory in cases where high strength is required. Furthermore, the biocompatibility is a requisite when the hydrogel is used in bio-related areas.

✉ Huijuan Zhang
zhanghuijuan@btbu.edu.cn

✉ Biao Yang
ybiao@btbu.edu.cn

[1] School of Materials Science and Mechanical Engineering, Beijing Technology and Business University, Beijing 100048, People's Republic of China

Polyvinyl alcohol (PVA) represents a type of a non-toxic, environmentally friendly, biodegradable, and water-soluble polymer, which is very suitable for the preparation of hydrogel by a simple process [33–39]. In some cases, physical method, i.e., freeze-thaw cycle, was preferred to cross-linked PVA hydrogels [40–43]. Ice crystal forms in the PVA solution when freezing, expelling PVA to phase-separate and promoting forming concentrated domains of PVA. After thawing these aggregated PVA, domains are free to form hydrogen bonds and crystals, and physically cross-linked gel is formed [44]. Based on freeze-thaw method, PVA-incorporated DN hydrogels showed high strength and functionality when combined with functional constituents [45–48]. Therefore, it is anticipated that the mechanical strength could be enhanced if PVA was incorporated into the nanocomposite system, by the freeze-thaw-induced physical cross-linking.

In this work, a tough PVA/Si/AM hydrogel with good recovery was reported which was prepared using VSNPs as multivalent covalent cross-linking agents and PVA hydrogen bonding and crystals as physical cross-linkers. The mechanical properties of the hydrogels were investigated by regulating the AM monomer, PVA, VSNPs concentrations, and the number of freeze-thaw cycles and freeze duration. The morphologies of the hydrogels were observed to show the topological variations when PVA experienced freeze-thaw cycle, with the aim to elucidate the microstructure evolution of the hydrogel. The loading-unloading tests were conducted to evaluate the energy dissipation of the PVA/Si/AM gels.

Experimental

Materials

Polyvinyl alcohol (PVA, with degree of polymerization of 1700 and alcoholysis degree 99%) was purchased from Changchun Chemical Co., Ltd. Acrylamide (AM), ammonium persulfate (APS), and N,N′-methylenebis-acrylamide (BIS) were purchased from Sinopharm Chemical Reagent, China. Vinyltriethoxysilane was purchased from Acros. All the reagents were used as received.

Preparation of PVA/PAM hydrogels cross-linked by vinyl-modified silica nanoparticles

Synthesis of VSNPs The vinyl hybrid silica nanoparticles were synthesized according to the literature [31, 32]. Typically, 3.8 g vinyltriethoxysilane was added into 30 g de-ionized water under vigorous stirring until the oil-like droplets completely disappeared. A transparent dispersion of vinyl-modified silica nanoparticles (VSNPs) was obtained after about 12 h.

Fabrication of nanocomposite hydrogels Nanocomposite hydrogels were prepared via a two-step method. Typically, 10 wt.% PVA aqueous solution was prepared by dissolving 10 g PVA into 90 g deionized water at 90 °C under stirring. The mixture solution was cooled to room temperature. Afterwards, 4 g AM and 5 mL 1.5 wt.% diluted aqueous VSNPs dispersion (weight percent with respect to AM) were added into 10 mL 10 wt.% PVA aqueous solution under vigorous stirring until the components were completely mixed. Then, 22 mg APS was added into the above solution and stirred for 30 min. Finally, the solution was transferred into a mold. The radical polymerization occurred at 60 °C for 6 h. In this step, a VSNPs cross-linked hydrogel was formed. Secondly, the VSNPs cross-linked hydrogel was frozen at − 20 °C for 6 h and then thawed at room temperature. The resulting hydrogel was then removed from the mold. A secondary network cross-linked due to the crystallization of PVA was formed under lower temperature. The general procedure used to prepare dual cross-linking hydrogels is illustrated in Fig. 1. The final products were denoted as PVAx-Siy-AMz, where x referred to the concentration of PVA aqueous solution, y referred to the weight percent of VSNPs relative to the weight of AM monomer, and z represented the weight of AM monomer. For comparison, the hydrogel cross-linked by chemical cross-linker was also prepared, which was denoted as PVAx-BISy-AMz. The detailed sample composition and preparation condition is shown in Table 1 as below.

Characterization The internal network structures of the hydrogels were characterized by scanning electron

Fig. 1 The size of the dumbbell-shaped hydrogel sample for tensile and hysteresis tests

Table 1 Sample composition of PVA-Si-AM hydrogels

Sample	PVA (wt.%)	VSNPs (wt.%)	AM (g)	BIS (g)	Freeze-thaw cycles	Freeze duration (h)
PVA10-Si0.5-AM2	10	0.5	2	0	1	6
PVA10-Si1-AM2	10	1.0	2	0	1	6
PVA10-Si1.5-AM2	10	1.5	2	0	1	6
PVA10-Si2-AM2	10	2.0	2	0	1	6
PVA8-Si1.5-AM2	8	1.5	2	0	1	6
PVA12-Si1.5-AM2	12	1.5	2	0	1	6
PVA15-Si1.5-AM2	15	1.5	2	0	1	6
PVA18-Si1.5-AM2	18	1.5	2	0	1	6
PVA18-Si1.5-AM3	18	1.5	3	0	1	6
PVA18-Si1.5-AM4	18	1.5	4	0	1	6
PVA18-Si1.5-AM4-0 h	18	1.5	4	0	1	0
PVA18-Si1.5-AM4-2 h	18	1.5	4	0	1	2
PVA18-Si1.5-AM4-4 h	18	1.5	4	0	1	4
PVA18-Si1.5-AM4-2FC	18	1.5	4	0	2	6
PVA18-BIS1.5-AM4	18	0	4	1.5	1	6

microscopy (SEM) (QUANTA FEG 250). Prior to the observation, the samples for SEM analysis were pretreated by freeze-drying technique. The tensile and hysteresis measurements of the hydrogels were conducted by using a TA.XT Plus texture analyzer (Stable Micro Systems, UK). The samples were cut into dumbbell shape, length 250 mm, width 4 mm, and gauge length 75 mm (shown in Fig. 1). The thickness of the hydrogel was measured using a caliper. Both ends of the dumbbell-shaped sample were connected to the clamps with the lower clamp fixed. The upper clamp was pulled by the load cell at a constant velocity of 60 mm min^{-1} at room temperature, by which the stress–strain curve was recorded and the experimental data was further analyzed. In a hysteresis measurement, a dumbbell-shaped sample was first elongated to a predetermined maximum stretch and then unloaded to zero force at a constant velocity of 60 mm min^{-1}. The dissipated energy for each cycle, ΔU, is defined as the area of hysteresis loop encompassed by the loading −unloading curve:

$$\Delta U = \int_{\text{loading}} \sigma d\varepsilon - \int_{\text{unloading}} \sigma d\varepsilon \quad (1)$$

Results and discussion

Synthesis and structure of the nanocomposite interpenetrating PVA-Si-AM hydrogels

For preparing nanocomposite PVA-Si-AM hydrogels, VSNPs were firstly synthesized by the hydrolysis of vinyltriethoxysilane via a sol-gel process. The vinyl-functionalized silica particles were then polymerized together with AM, in the presence of PVA, to form a VSNPs-cross-linked PVA-Si-AM nanocomposite network. The PAM polymer chains were covalently cross-linked by the VSNPs with

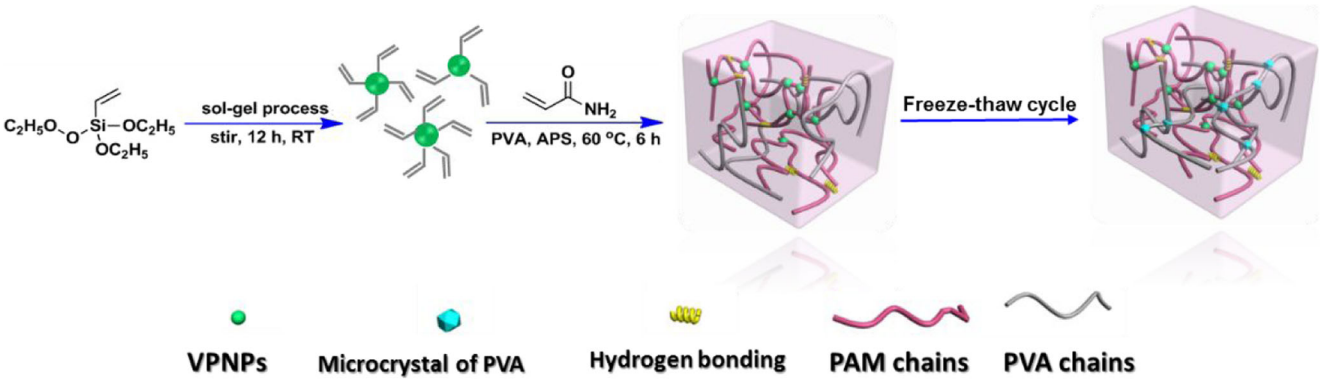

Scheme 1 Schematic preparation process of nanocomposite interpenetrating hydrogel

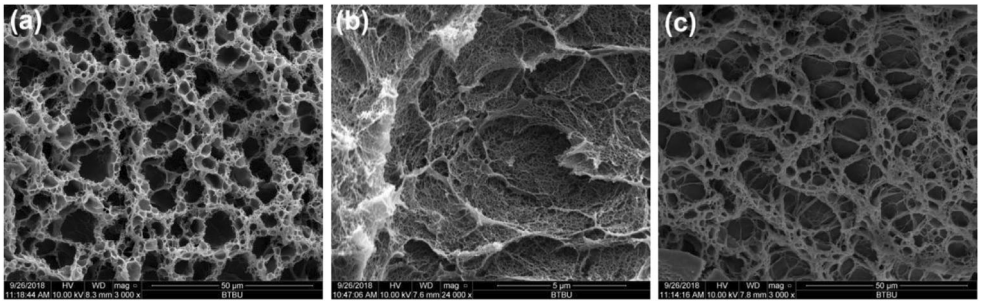

Fig. 2 SEM images of the PVA18-Si1.5-AM4 hydrogel **a** with one freeze-thaw cycle, **b** no freeze-thaw cycle, **c** PVA18-BIS1.5-AM4 hydrogel with one freeze-thaw cycle

PVA chains interpenetrating in the network. Afterwards, a freeze-thaw cycle was conducted to form a secondary physical cross-linking induced by the crystallization of PVA in the process (Scheme 1). There are two types of cross-linking in the hydrogel: one is the strong covalent bonding between PAM chains and VSNPs, and the other is the physical cross-linker induced by hydrogen bonding in both PAM chains and PAM chains and hydroxyl groups on PVA, as well as PVA microcrystals. Combining the dual nanocomposite and physical cross-linking, the hydrogel exhibited following advantages: (1) VSNPs could strengthen the hydrogel by dissipating energy and homogenize the PAM network under large strain; (2) the physical cross-linking formed by hydrogen bonding, both in PAM chains and PAM chains and hydroxyl groups on PVA, and microcrystals in PVA provide sacrificial bonds during stretching, which could dynamically rearrange to dissipate energy and recover rapidly; (3) the crystallized PVA chains tend to orient during stretching which would produce higher strength after loading-unloading cycles.

The nanocomposite interpenetrating hydrogel exhibited a typical porous morphology as shown in Fig. 2a. Hierarchical porous structure can be observed for the hydrogel after one freeze-thaw cycle. The network was characterized by the pores of 10~20 μm interconnected by the smaller pores of 0.7~1 μm. The as-prepared nanocomposite hydrogel without freeze-thaw cycle displayed a diverse morphology (Fig. 2b). The network was composed of micropores of 3~10 μm and nanopores with pore size of about 500 nm. In other words, the microstructure of the hydrogel without experiencing freeze-thaw cycle was at a smaller size level. As reported previously [49], the LDH/PAM NC hydrogels with a network at both micro- and nanometer (less than 500 nm) scales showed a high tensibility. The current work indicated a different trend, that is, the network with a nanoscale microstructure showed a lower strength (discussed in the following sections). It seems that the hydrogel after freeze-thaw cycle underwent a "grow-up and rearrange" process. To be specific, ice crystal formed in the PVA18-Si1.5-AM4 hydrogel when freezing, expelling PVA to phase-separate and promoting the formation of concentrated domains of PVA. After thawing these aggregated PVA domains are free to form hydrogen bonds and crystals, and physical cross-linker was formed. The PVA chains in the network existed as a more aggregated and ordered form, which connected with each other and constituted a network with larger pore size. The "grow-up" process was supposed to form a more stable network, enabling the hydrogel to display higher strength. A PVA18-BIS1.5-AM4 hydrogel was also prepared, in which VSNPs cross-linker was replaced by the BIS chemical cross-linker, and the SEM image was illustrated in Fig. 2c. The BIS-cross-linked hydrogel exhibited a similar microstructure to that of the VSNPs-cross-linked one, with a hierarchy of porous morphology. The analogy in morphology was probably due to the reason that the VSNPs and BIS cross-linkers are chemical in nature, and the polymerization occurred in a similar way, which would produce similar microstructures of the hydrogels.

Mechanical properties of the PVA-Si-AM hydrogels

Taking advantage of the nanocomposite and physical network architecture, the as-prepared hydrogel cross-linked by VSNPs outperformed the BIS-cross-linked counterpart. For example, PVA18-BIS1.5-AM4 was merely 1.05 MPa in tensile strength at the strain of 208%. In contrast, PVA18-Si1.5-AM4 sample showed a tensile stress of 1.62 MPa, which was 1.5 times

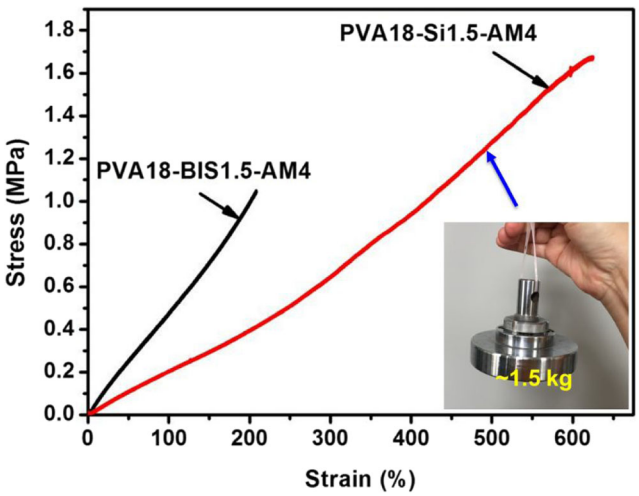

Fig. 3 Tensile stress-strain curve of PVA18-Si1.5-AM4 and PVA18-BIS1.5-AM4. Inset shows the PVA18-Si1.5-AM4 hydrogel can lift a steel block of ~ 1.5 kg in weight

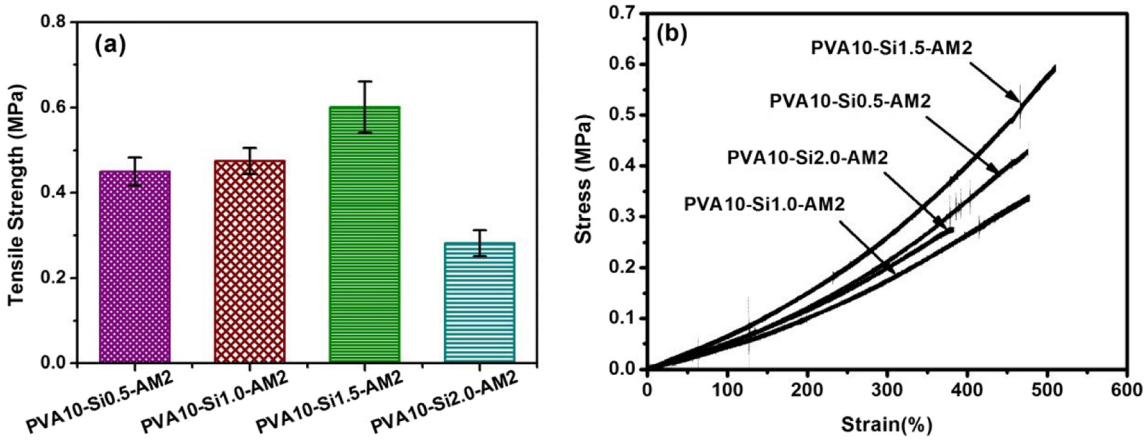

Fig. 4 **a** Tensile strength and **b** stress-strain curve of the PVA10-Si-AM2 hydrogels with varying VSNPs contents

higher than that of PVA18-BIS1.5-AM4, and the corresponding strain was 625%, also 3 times higher than that of PVA18-BIS1.5-AM4 (Fig. 3). The VSNPs-cross-linked gel could sustain a steel block of ~ 1.5 kg in weight, exhibiting its excellent toughness (Fig. 3 inset). The results demonstrated the superiority of VSNPs as a cross-linker, which could dissipate energy more effectively when being stretched and exhibited more pronounced tensile performance.

For PVA-Si-AM hydrogels, further investigation was performed to study the effect of the concentrations of VSNPs, PVA, and AM on tensile mechanical properties of the PVA-Si-AM hydrogels as shown in Figs. 4, 5, and 6. Tensile stress-strain curve and tensile strength of the PVA-Si-AM hydrogels with varying VSNPs contents were presented in Fig. 4. The VSNPs concentration was determined relative to the weight of AM monomer to be 0.5, 1, 1.5, and 2 wt%, respectively. The hydrogel with 0.5 wt% VSNPs was 0.449 MPa in tensile strength (Fig. 4a) with a 476% stain (Fig. 4b). The strength went up with further increase of the VSNPs content, and an optimized strength was obtained when the concentration was 1.5 wt%. The strain was 511% at this content. When the VSNPs weight percent was raised to 2 wt%, the tensile strength was lowered to be 0.282 MPa with a 383% strain. The VSNPs concentration exerted a twofold influence on the tensile strength both as a cross-linker and nano-reinforcement. On the one hand, the vinyl groups in VSNPs acted as a chemical cross-linker to cross-link the PAM polymer chains. More cross-linkers tended to produce a network with a higher cross-linking density and strengthened the hydrogel. On the other hand, the nanoparticles can serve as reinforcement which dissipated energy when stretching. At higher weight ratio, i.e., 2 wt%, the nanoparticles may aggregate to a certain extent and the strengthening role abated greatly, which resulted in a weak hydrogel.

Keeping the VSNPs concentration to be 1.5 wt% and AM to be 2 g, the PVA amount was optimized and the results were presented in Fig. 5. When PVA concentration was varied between 8, 10, 12, 15, and 18 wt%, the tensile strength showed a continuing increase from 0.392 to as high as 1.63 MPa (Fig. 5a). Meanwhile, the hydrogel with 18 wt% PVA incorporation exhibited a higher 600% strain (Fig. 5b), demonstrating its superior toughness. Microcrystals would form in PVA when

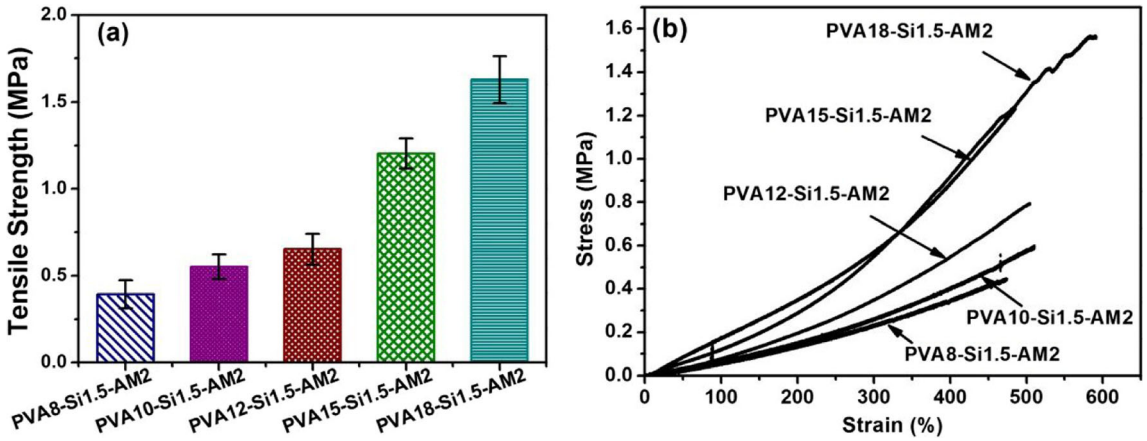

Fig. 5 **a** Tensile strength and **b** tensile stress-strain curve of the PVA-Si1.5-AM2 hydrogels with varying PVA concentrations

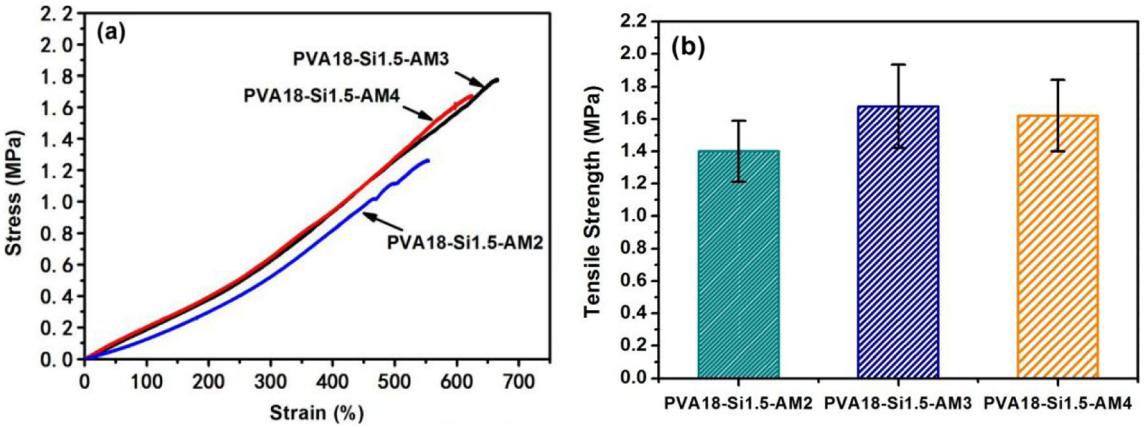

Fig. 6 Tensile stress-strain curve **a** and **b** tensile strength of the PVA18-Si1.5-AM hydrogels with varying AM weights

PVA18-Si1.5-AM2 was freezing, expelling PVA to phase-separate and promoting forming concentrated domains of PVA. After thawing the aggregated PVA domains are free to form hydrogen bonds and crystals, and physical cross-linker is thus produced. On the other hand, the hydrogen bonding in both PAM chains and PAM chains and hydroxyl groups on PVA also served as physical cross-linkers. The physical cross-linker served as sacrificial bonds during stretching, which could dynamically rearrange to dissipate energy to produce a tough hydrogel.

For PVA18-Si1.5-AM gels, further investigation was performed to study the effect of AM monomer content on the tensile mechanical properties. As shown in Fig. 6, the AM concentration had a less significant influence on the tensile properties with the tensile strength of 1.40~1.67 MPa for the three samples, i.e., with AM content of 2 g, 3 g, and 4 g, respectively. The overall trend is that the tensile strength increased with when the AM content went up and then fell down with the further increasing AM. The reason may be that when the AM content reached a threshold value, the PAM chains was enough to construct the network and form the hydrogen bonding. The tensile strength cannot be further elevated purely by raising the AM content. Instead, an overdose of AM may cause the unevenness of the network and the decline of the strength.

The influences of the number of freeze-thaw cycles and the freeze duration of PVA-Si-AM were also studied as presented in Fig. 7. PVA18-Si1.5-AM4 gel without experiencing freeze-thaw cycle had tensile strength of only 0.574 MPa, while the sample with one freeze-thaw cycle had a much higher tensile strength of 1.67 MPa (Fig. 7). The enhanced network of PVA with crystalline microdomains should be responsible for the improvement. By subjecting the gel to two cycles of freezing/thawing procedure, however, the tensile strength (1.69 MPa) did not vary much. Moreover, the duration time exerted a lesser influence on the tensile properties of the gel. And the gels with different freeze-thaw duration, i.e., 2, 4 or 6 h, presented a tensile strength of 1.92, 1.71, and 1.88 MPa. The reason may be that the PVA/Si/AM hydrogel with physical and nanocomposite architecture was endowed with a stable architecture, in which PVA polymer chains interpenetrating in the VSNPs-cross-linked network with less flexibility. Varying the freeze-thaw cycle numbers or duration can hardly produce a notable effect on the inner structure and the mechanical properties of the gel.

Toughness, self-recovery, and draw-induced toughening of PVA-Si-AM gel

Toughness of hydrogels usually offers remarkable dissipation of energy, which is of great importance to be practical application [50]. In view of this, cyclic tensile loading-unloading tests were carried out to evaluate the energy dissipation as shown in Figs. 8, 9, and 10, which could be calculated from the strain hysteresis curves. The

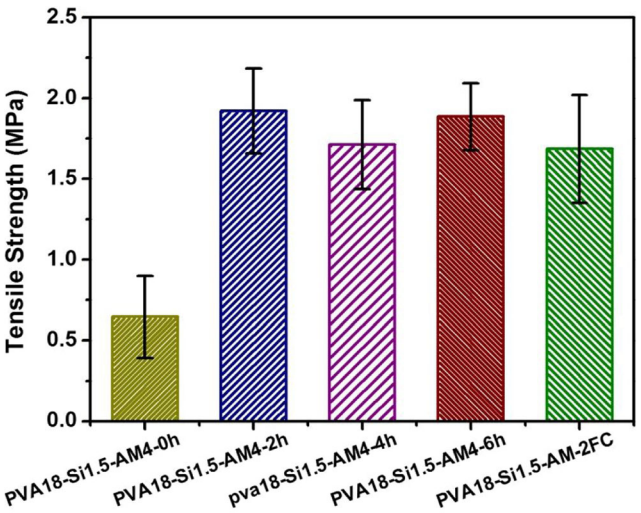

Fig. 7 Tensile stress-strain curve of PVA18-Si1.5-AM4 hydrogel with different freeze duration and freeze-thaw cycles

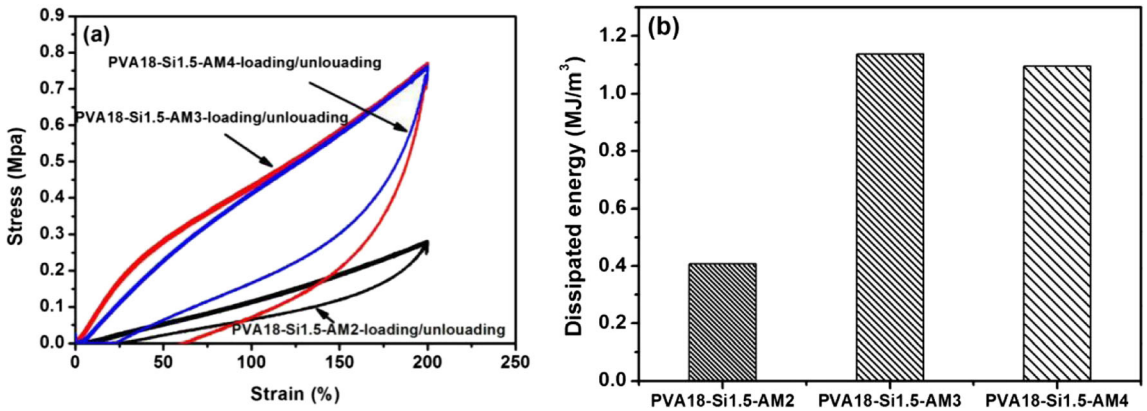

Fig. 8 **a** Loading-unloading tests of the PVA18-Si1.5-AM hydrogels under 200% strain, **b** the calculated dissipated energy of PVA18-Si1.5-AM hydrogels under 200% strain

pronounced hysteresis in Fig. 8a suggested that PVA18-Si1.5-AM gels could effectively dissipate energy, and the hysteresis loop become bigger at higher AM content. A quantified data for the fracture energy of the PVA18-Si1.5-AM gels with increasing AM concentrations was illustrated in Fig. 8b. At a 200% strain, PVA18-Si1.5-AM2, PVA18-Si1.5-AM3, and PVA18-Si1.5-AM4 indicated a dissipated energy of 0.408, 1.14, and 1.09 MJ/m^3, respectively. The data supported the trend of the tensile strength shown in Fig. 6, demonstrating the superior energy capacity of PVA18-Si1.5-AM4.

PVA18-Si1.5-AM4 hydrogels showed good self-recovery and draw-induced toughening. After 30 min of resting, the dissipated energy of the gels restored from 1.05 to 1.06 MJ/m^3 after the second cycle (Fig. 9b). This could probably be ascribed to the physically reversible cross-linking in the network, which could be reformed when the external force was withdrawn. It is interesting to find that the tensile strength and dissipated energy of the gel increased after the loading-unloading cycles. As depicted in Fig. 8a, the tensile stress went up from 0.65 to 0.73 MPa after the first cycle. And the corresponding dissipated energy was 1.05 and 1.06 MJ/m^3, respectively (Fig. 9b). When the gel was subject to the third tensile cycle 30 min later, the tensile strength was further raised to 0.92 MPa, and the dissipated energy of 1.18 MJ/m^3 was obtained. The draw-induced toughening of the gels was probably related to the draw orientation of PVA, which frequently occurred in polymer chains when being stretched. In the process, PVA chain extension and molecular orientation would take place along the stretching direction, and the oriented polymer chains can be stabilized in the unloading process. The tensile strength was thus be elevated after loading-unloading process.

The gel indicated a time-dependent self-recovery phenomenon. Figure 10 showed the loading-unloading curves of PVA18-Si1.5-AM4 gel when being conducted loading-unloading cycling tests at 100, 200, and 300% strains without rest. Obvious strain relaxation can be observed after the second and third cycling tests. And the gel became softened and weakened with the increasing loading-unloading cycles. In other words, the self-recovery of the gel was time-dependent. It can be explained as follows: substantial physical cross-linkers in the network were cracked after being stretched. When being stretched immediately, it is too soon for the gel

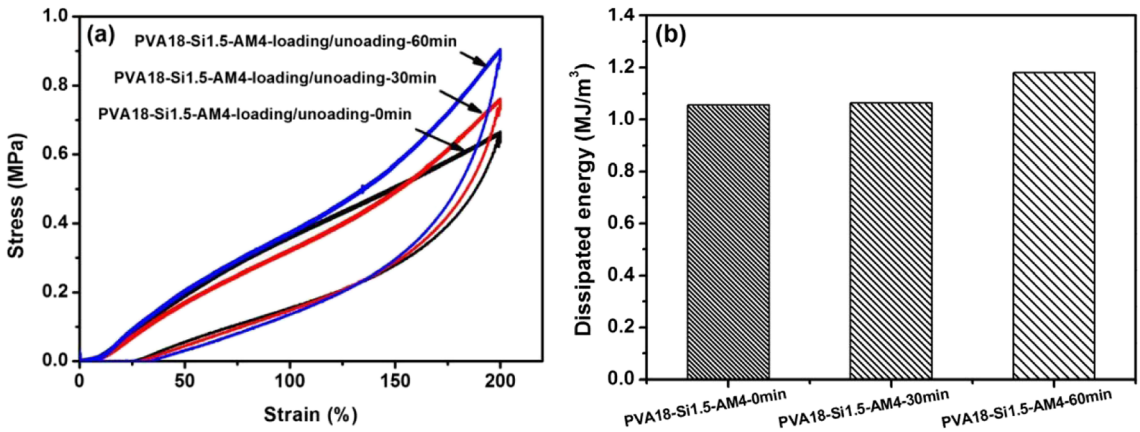

Fig. 9 **a** Three successive loading−unloading cycling test of PVA18-Si1.5-AM4 hydrogel at a strain of 200% with 30 min resting between two tests, **b** the time-dependent recovery of dissipated energy of PVA18-Si1.5-AM4 hydrogel

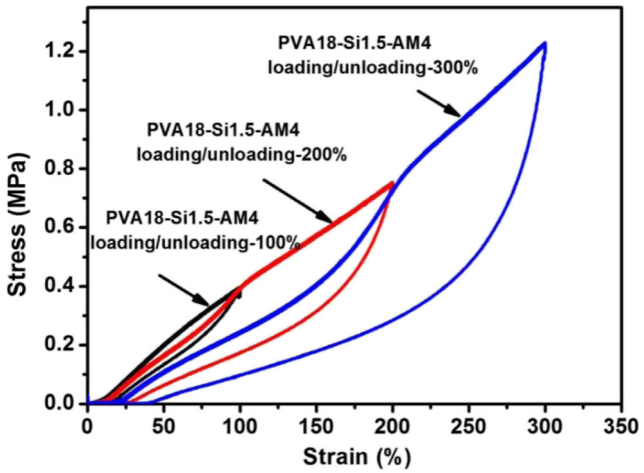

Fig. 10 Loading-unloading cycling tests of PVA18-Si1.5-AM4 hydrogel at different strains

to restore the bonding, resulting in the obvious stress relaxation of the gel.

Toughening mechanism of the nanocomposite interpenetrating gels

Obviously, the nanocomposite interpenetrating gels showed superior mechanical properties, particularly toughness and self-recovery, and draw-induced strengthening phenomenon. The remarkable enhancement of the gels could be explained in terms of their unique network structure and effective strengthening mechanism as shown in Scheme 2. In the relaxed state, the polymer chains in the nanocomposite interpenetrating gels were supposed to adopt random coil conformations. The network was linked through the VSNPs covalent cross-linking, hydrogen bonding and PVA microcrystals (Scheme 2a). Upon stretching, the energy was dispersed through the network by the uncoiling of the polymer chains and the aid of the VSNPs. With the further increase of tension force, it was difficult to unentangle the chains, and the energy was dissipated through the fracture of the reversible physical cross-links. Meanwhile, PVA polymer chains exhibited draw-induce orientation along the external force direction in the process (Scheme 2b). The physical interactions could reform and resulted in a more homogenized network. The dynamic nature of the physical interaction endowed the gels with good self-recovery property. The PVA orientation was maintained to a great extent after the external force was withdrawn, which gave rise to a draw-induced toughening of the gel (Scheme 2c) when the gel was subjected to the second and third loading-unloading cycles.

Conclusions

In summary, we report a feasible method to construct nanocomposite interpenetrating hydrogels with VSNPs as nano-cross-linkers and PVA hydrogen bonding and microcrystalline

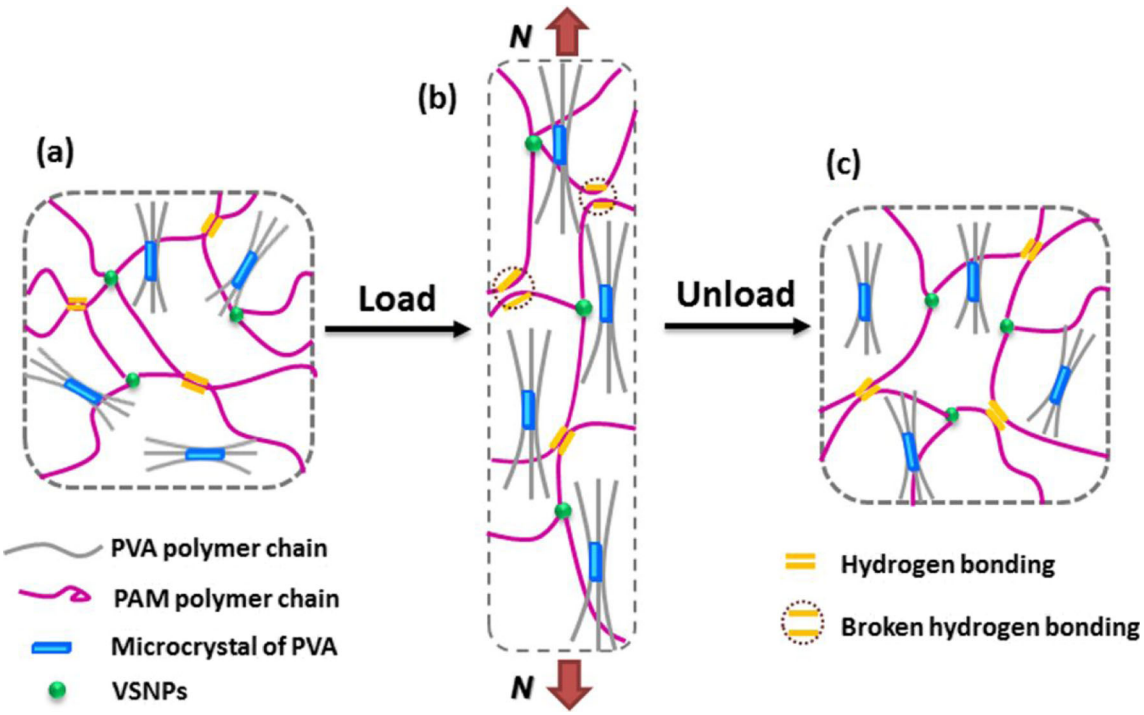

Scheme 2 Schematic illustration of the structural change and the toughening mechanism of the nanocomposite interpenetrating cross-linking gel when stretching

as physical cross-linkers formed by simple freeze-thaw post-treatment. Aided by the nano-reinforcement and the physical cross-linker, the gels possessed high tensile strength, high toughness, and good self-recovery. The outstanding mechanical properties of the nanocomposite interpenetrating hydrogels originated from synergetic interactions of physical cross-linkings and VSNPs nano-network, wherein the disruption of physical cross-linkings effectively dissipated energy while the VSNPs homogenized the network during deformation process. Notably, reversible reorganization and draw orientation of PVA physical networks empowered the nanocomposite interpenetrating hydrogels rapid self-recovery and draw-induced toughening abilities.

Funding information We acknowledge financial support from the National Nature Science Foundation of China (No. 21104040, 51473007, 31570575).

Compliance with ethical standards

Conflict of interest The authors declare that they have no conflict of interest.

References

1. Chang G, Chen Y, Li Y, Li S, Huang F, Shen Y, Xie A (2015) Self-healable hydrogel on tumor cell as drug delivery system for localized and effective therapy. Carbohydr Polym 122:336–342
2. Chen C, Zhang T, Dai B, Zhang H, Chen X, Yang J, Liu J, Sun D (2016) Rapid fabrication of composite hydrogel microfibers for weavable and sustainable antibacterial applications. ACS Sustain Chem Eng 4:6534–6542
3. Lee KY, Mooney DJ (2001) Hydrogels for tissue engineering. Chem Rev 101(7):1869–1879
4. Appel EA, del Barrio J, Loh XJ, Scherman OA (2012) Supramolecular polymeric hydrogels. Chem Soc Rev 41(18): 6195–6214
5. Hu J, Kurokawa T, Hiwatashi TK, Nakajima T, Wu ZL, Liang SM, Gong JP (2012) Structure optimization and mechanical model for microgel-reinforced hydrogels with high strength and toughness. Macromolecules 45:5218–5228
6. Hu J, Hiwatashi K, Kurokawa T, Liang SM, Wu ZL, Gong JP (2011) Microgel-reinforced hydrogel films with high mechanical strength and their visible mesoscale fracture structure. Macromolecules 44:7775–7781
7. Gao GR, Du GL, Cheng YJ, Fu J (2014) Tough nanocomposite double network hydrogels reinforced with clay nanorods through covalent bonding and reversible chain adsorption. J Mater Chem B 2:1539–1549
8. Aranaz I, Martínez-Campos E, Nash ME, Tardajos MG, Reinecke H, Elvira C, Ramos V, López-Lacomba JL, Gallardo A (2014) Pseudo-double network hydrogels with unique properties as supports for cell manipulation. J Mater Chem B 2:3839–3848
9. Yin HY, Akasaki T, Sun TL, Nakajima T, Kurokawa T, Nonoyama T, Taira T, Saruwatari Y, Gong JP (2013) Double network hydrogels from polyzwitterions: high mechanical strength and excellent anti-biofouling properties. J Mater Chem B 1:3685–3693
10. Ito K (2007) Novel cross-linking concept of polymer network: synthesis, structure, and properties of slide-ring gels with freely movable junctions. Polym J 39:489–499
11. Haraguchi K, Takehisa T, Fan S (2002) Effects of clay content on the properties of nanocomposite hydrogels composed of poly(N-isopropylacrylamide) and clay. Macromolecules 35:10162–10171
12. Zhu MF, Liu Y, Sun B, Zhang W, Liu XL, Yu H, Zhang Y, Kuckling D, Adler HP (2006) A novel highly resilient nanocomposite hydrogel with low hysteresis and ultrahigh elongation. Macromol Rapid Commun 27:1023–1028
13. Kostina NY, Sharifi S, Pereira AS, Michálek J, Grijpma DW, Rodriguez-Emmenegger C (2013) Novel antifouling self-healing poly(carboxybetaine methacrylamide-co-HEMA) nanocomposite hydrogels with superior mechanical properties. J Mater Chem B 1:5644–5650
14. Li ZY, Su YL, Xie BQ, Wang HL, Wen T, He CC, Shen H, Wu DC, Wang DJ (2013) A tough hydrogel–hydroxyapatite bone-like composite fabricated in situ by the electrophoresis approach. J Mater Chem B 1:1755–1764
15. Sun JY, Zhao XH, Illeperuma WRK, Chaudhuri O, Oh KH, Mooney DJ, Vlassak JJ, Suo ZG (2012) Highly stretchable and tough hydrogels. Nature 489:133–136
16. Li JY, Suo ZG, Vlassak JJ (2014) Stiff, strong, and tough hydrogels with good chemical stability. J Mater Chem B 2:6708–6713
17. Yang YY, Wang X, Yang F, Shen H, Wu DC (2016) A universal strategy to convert composite hydrogels into extremely tough and rapidly recoverable double-network hydrogels. Adv Mater 28: 7178–7184
18. Zhang HJ, Cheng YR, Hou XJ, Yang B, Guo F (2018) Ionic effects on the mechanical and swelling properties of a poly(acrylic acid/acrylamide) double crosslinking hydrogel. New J Chem 42: 9151–9158
19. Kong WQ, Wang CW, Jia C, Kuang YD, Pastel G, Chen CJ, Chen G, He SM, Huang H, Zhang JH, Wang S, Hu LB (2018) Muscle-inspired highly anisotropic, strong, ion-conductive hydrogels. Adv Mater 30: 1801934
20. Peak CW, Wilker JJ, Schmidt G (2013) Review on tough and sticky hydrogels. Colloid Polym Sci 291:2031–2047
21. Duan JJ, Zhang LN (2017) Robust and smart hydrogels based on natural polymers. Chin J Polym Sci 35:1165–1180
22. Fan HL, Wang JH, Jin ZX (2018) Tough, swelling-resistant, self-healing, and adhesive dual-cross-linked hydrogels based on polymer−tannic acid multiple hydrogen bonds. Macromolecules 51: 1696–1705
23. Yao C, Liu Z, Yang C, Wang W, Ju XJ, Xie R, Chu LY (2015) Poly(N-isopropylacrylamide)-clay nanocomposite hydrogels with responsive bending property as temperature-controlled manipulators. Adv Funct Mater 25:2980–2991
24. Haraguchi K (2011) Synthesis and properties of soft nanocomposite materials with novel organic/inorganic network structures. Polym J 43:223–241
25. Xiong L, Hu X, Liu X, Tong Z (2008) Network chain density and relaxation of in situ synthesized polyacrylamide/hectorite clay nanocomposite hydrogels with ultrahigh tensibility. Polymer 49: 5064–5071
26. Su X, Chen BQ (2018) Tough, resilient and pH-sensitive interpenetrating polyacrylamide/alginate/montmorillonite nanocomposite hydrogels. Carbohydr Polym 197:497–507
27. Liu RQ, Liang SM, Tang XZ, Yan D, Li XF, Yu ZZ (2012) Tough and highly stretchable graphene oxide/polyacrylamide nanocomposite hydrogels. J Mater Chem 22:14160–14167
28. Liu J, Song G, He C, Wang H (2013) Self-healing in tough graphene oxide composite hydrogels. Macromol Rapid Commun 34:1002–1007
29. Zhang HJ, Zhai DD, He Y (2014) Graphene oxide/polyacrylamide/carboxymethyl cellulose sodium nanocomposite hydrogel with

enhanced mechanical strength: preparation, characterization and the swelling behavior. RSC Adv 4:44600–44609
30. Lin WC, Fan W, Marcellan A, Hourdet D, Creton C (2010) Large strain and fracture properties of poly(dimethylacrylamide)/silica hybrid hydrogels. Macromolecules 43(5):2554–2563
31. Shi FK, Wang XP, Guo RH, Zhong M, Xie XM (2015) Highly stretchable and super tough nanocomposite physical hydrogels facilitated by the coupling of intermolecular hydrogen bonds and analogous chemical crosslinking of nanoparticles. J Mater Chem B 3:1187–1192
32. Zhong M, Liu XY, Shi FK, Zhang LQ, Wang XP, Cheetham AG, Cui HG, Xie XM (2015) Self-healable, tough and highly stretchable ionic nanocomposite physical hydrogels. Soft Matter 11:4235–4241
33. Han J, Lei T, Wu Q (2014) High-water-content mouldable polyvinylalcohol-borax hydrogels reinforced by well-dispersed cellulose nanoparticles: dynamic rheological properties and hydrogel formation mechanism. Carbohydr Polym 102:306–316
34. Wang Z, Tao F, Pan Q (2016) A self-healable polyvinyl alcoholbased hydrogel electrolyte for smart electrochemical capacitors. J Mater Chem A 4:17732–17739
35. Liu K, Pan XF, Chen LH, Huang LL, Ni YH, Liu J, Cao SL, Wang HP (2018) Ultrasoft self-healing nanoparticle-hydrogel composites with conductive and magnetic properties. ACS Sustain Chem Eng 6:6395–6403
36. Ou KK, Dong X, Qin CL, Ji XN, He JX (2017) Properties and toughening mechanisms of PVA/PAM double-network hydrogels prepared by freeze-thawing and anneal-swelling. Mater Sci Eng C 77:1017–1026
37. Fernández E, López D, López-Cabarcos E, Mijangos C (2005) Viscoelastic and swelling properties of glucose oxidase loaded polyacrylamide hydrogels and the evaluation of their properties as glucose sensors. Polymer 7:2211–2217
38. Yao W, Geng C, Han D, Chen F, Fu Q (2014) Strong and conductive double-network graphene/PVA gel. RSC Adv 74:39588–39595
39. Chu L, Liu C, Zhou G, Xu R, Tang YH, Zeng ZB, Luo SL (2015) A double network gel as low cost and easy recycle adsorbent: highly efficient removal of Cd (II) and Pb (II) pollutants from wastewater. J Hazard Mater 300:153–160
40. Bodugoz-Senturk H, Macias CE, Kung JH, Muratoglu OK (2009) Poly (vinyl alcohol)-acrylamide hydrogels as load-bearing cartilage substitute. Biomaterials 30:589–596
41. Park KR, Nho YC (2003) Synthesis of PVA/PVP hydrogels having two-layer by radiation and their physical properties. Radiat Phys Chem 67:361–365
42. Mansur HS, Sadahira CM, Souza AN, Mansur AAP (2008) FTIR spectroscopy characterization of poly (vinyl alcohol) hydrogel with different hydrolysis degree and chemically crosslinked with glutaraldehyde. Mater Sci Eng C 28:539–548
43. Liu Y, Vrana N, Cahill P, Mcguinness GB (2009) Physically crosslinked composite hydrogels of PVA with natural macromolecules: structure, mechanical properties, and endothelial cell compatibility. J Biomed Mater Res B Appl Biomater 90:492–502
44. Hatakeyema T, Uno J, Yamada C, Kishi A, Hatakeyama H (2005) Gel-sol transition of poly(vinyl alcohol) hydrogels formed by freezing and thawing. Thermochim Acta 431:144–148
45. Lu X, Hu CX, Zhang YL, Wang XD, Shi LY, Ran R (2019) A mechanically robust double-network hydrogel with high thermal responses via doping hydroxylated boron nitride nanosheets. J Mater Sci 54:3368–3382
46. Zhou Y, Wan CJ, Yang YS, Yang H, Wang SC, Dai ZD, Ji KJ, Jiang H, Chen XD, Long Y (2019) Highly stretchable, elastic, and ionic conductive hydrogel for artificial soft electronics. Adv Funct Mater 29:1806220
47. Shih CC, Wu M, Hsu SN, Huang CW, Hsu LC, Lam JY, Chen WC (2018) A robust, air-stable and recyclable hydrogel toward stretchable electronic device applications, 303: 1800282
48. Wang S, Zhang Z, Chen B, Shao J, Guo ZY (2018) Self-healing hydrogel of poly(vinyl alcohol)/graphite oxide with pH-sensitive and enhanced thermal properties. J Appl Polym Sci 135:46143
49. Hu ZQ, Chen GM (2014) Novel nanocomposite hydrogels consisting of layered double hydroxide with ultrahigh tensibility and hierarchical porous structure at low inorganic content. Adv Mater 26:5950–5956
50. Gong ZY, Zhang GP, Zeng XL, Li JH, Li G, Huang WP, Sun R, Wong CP (2016) High-strength, tough, fatigue resistant, and self-healing hydrogel based on dual physically cross-linked network. ACS Appl Mater Interfaces 8:24030–24037